

EXPERIMENTAL VALIDATION OF THE DYNAMIC FINITE ELEMENT MODEL OF A 1:8 SCALE SEAPLANE USING A LASER DOPPLER VIBROMETER (LDV)

F. Lovero¹, G. Biggi¹, S. Lombardi¹, M.A.C. Costa¹, V. Amore¹ & E. Cestino¹

¹Department of Mechanical and Aerospace Engineering, Politecnico di Torino, Turin, Italy

Abstract

This study presents a comprehensive analysis of Ground Vibration Tests (GVT) and Finite Element Method (FEM) simulations conducted on a full composite seaplane scaled model. The objective is to evaluate the dynamic behavior of the seaplane. Ground vibration tests were performed to measure the natural frequencies and mode shapes of the aircraft structure by means of the innovative Laser Doppler Vibrometer (LVD) technique. Concurrently, a detailed finite element model was developed, incorporating the material properties and geometric configurations specific to the composite construction of the seaplane. The comparison revealed good agreement in the lower frequency modes.

Keywords: Seaplane, Modal Analysis, Frequency, Laser Doppler Vibrometer, Shaker

1. Introduction

Team S55 is a team from *Politecnico di Torino* aiming to construct a 1:8 scale flying replica of the *Savoia-Marchetti S55-X* (Figure 1), an Italian seaplane from the 1920s [1] [2]. Initially, they've researched the historical model, enhancing it with contemporary techniques and resources through collaboration with external engineering experts and industries.



Figure 1 – 1:8 Scale Replica of S55 Seaplane

Aeronautical structures are composed of various components that distribute the loads they sustain [3]. During its operational life, the aircraft encounters several types of dynamic loads and a dynamic and an aeroelastic verification is crucial to ensure aircraft structural integrity. The test article (Figure 2) encompasses the configuration considered for this test and includes the following components:

- · Complete wing with controls and receiver;
- Central wing box with engine mount, fairing, engines, and propellers;
- · Hulls with batteries.

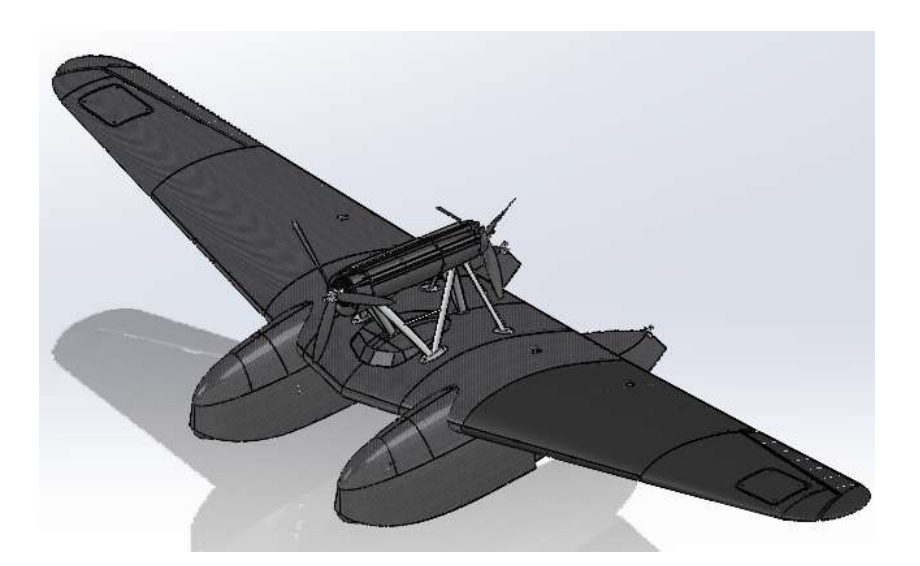


Figure 2 – Test Article

In this study, the scaled model seaplane is being analyzed with the aim of elucidating and comprehending the modal behavior of the structure [4]. The methodology employed relies on the application of the Finite Element Method to execute a free-free modal analysis of the test article, following three steps: pre-processing, processing, and post-processing. The pre-processing part can be carried out using a software called ANSA by BetaCAE Systems. In this phase, the seaplane geometry is imported from the CAD, cleaned-up, meshed and the non structural masses and the internal component connections are added. The processing, which is the actual calculation step, is performed using the Nastran solver. Specifically, SOL103 is used to execute the modal analysis. In the end the post-processing phase is carried out using the software META by BetaCAE Systems, that allows to visualize the calculated modal shapes.

The FEM model allows to obtain a mathematical model that represents the structure and the results of natural vibrations, showing the possibles behaviors that the seaplane could have. The numerical analysis of natural frequencies and modes of vibration, obtained through the FEM, is subsequently validated through experimental tests. In order to simulate the free-free condition, the seaplane model is suspended with elastic bands and excited with a shaker. For measuring modal shapes the experimental tests are conducted utilizing a Laser Doppler Vibrometer, one of the most advanced and accurate instruments currently available on the market for tests of this kind.

2. FE model

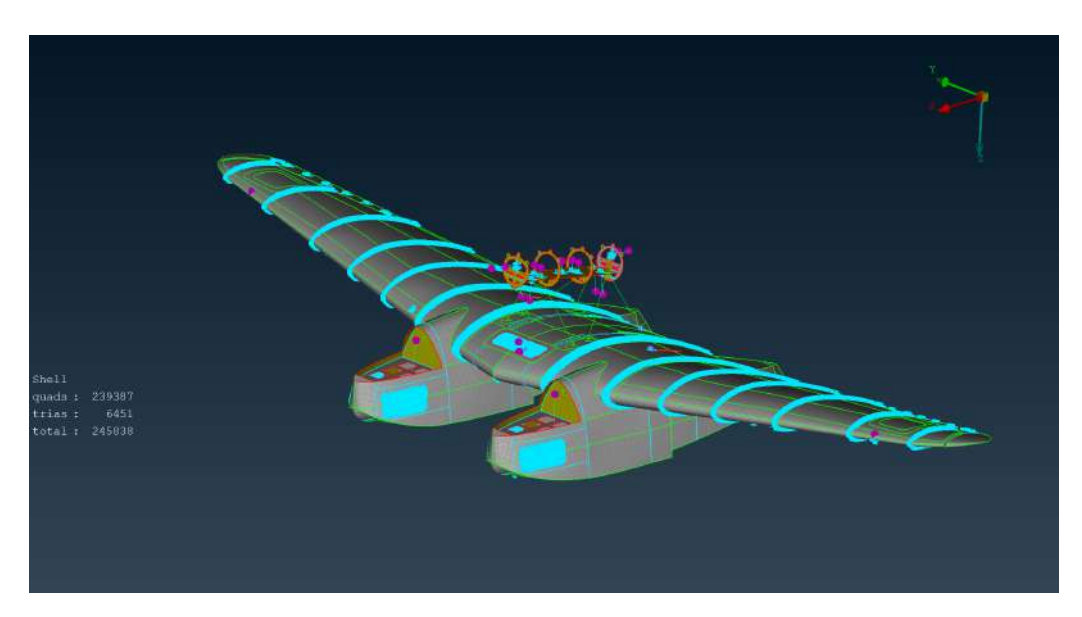


Figure 3 – FE Model of the Seaplane

The seaplane, illustrated in Figure 3, is modelled using BetaCAE Systems's software, ANSA. The first step of the process, consists in importing the CAD file of the model after which the geometry cleanup is carried out. This involves connecting surfaces, closing gaps between them, and optimizing the contours and faces in order to create the most regular mesh elements possible, avoiding the presence of complex surfaces, by optimizing the entire geometry.

The next step is the creation of the mesh. Mesh can vary in complexity and density depending on the requirements of the simulation and the level of detail needed to accurately capture the behavior of the system. In this case, an hybrid mesh composed of QUAD4 and TRIA3 shell elements is used for most of the structure. Shell elements used to have dimensions ranging from 2mm to 5mm in accordance with the geometry fraction they have to discretize.

The support beams of the engine mount are the only structural components discretized differently: 1D ROD elements are used (shown in green in Figure 4).



Figure 4 – ROD Connecting the Wing Box to the Engine Mount

The following couples of components are connected between them using rigid RBE2 connections:

- · Wing shell ribs;
- Ribs spars;

- · Wing hull;
- · Hull central wing box.

At this stage, it is possible to apply properties to all the elements of the model. The seaplane is manufactured using different techniques and materials. The materials of the main structural components are listed in Table 1.

Parts	Description	Materials	
Wing	Skin	Carbon fiber, Rohacell	
VVIIIg	Ribs, Spars	Carbon fiber	
Hulls	Superior Skin	Carbon fiber, Rohacell	
Tiulis	Inferior Skin	Glass fiber, Kevlar fiber, Carbon-Kevlar fiber, Rohacell	
Central Wing Box	Skin, Ribs	Carbon fiber, Rohacell	
Central Wing Box	Spars	Carbon fiber	

Table 1 - Constituent Materials

2.1 Static Validation



Figure 5 – Static Experimental Test

Once the FE model is created, it is necessary to validate it through experimental tests [3]. The first and easiest test that ensures some level of compatibility between model and real seaplane is a static stiffness test.

Downward forces are applied to the the front and the rear part of each hull while vertical translations are blocked beneath the wing. The constraints and forces replicate the real ones used during the experimental test, shown in Figure 5.

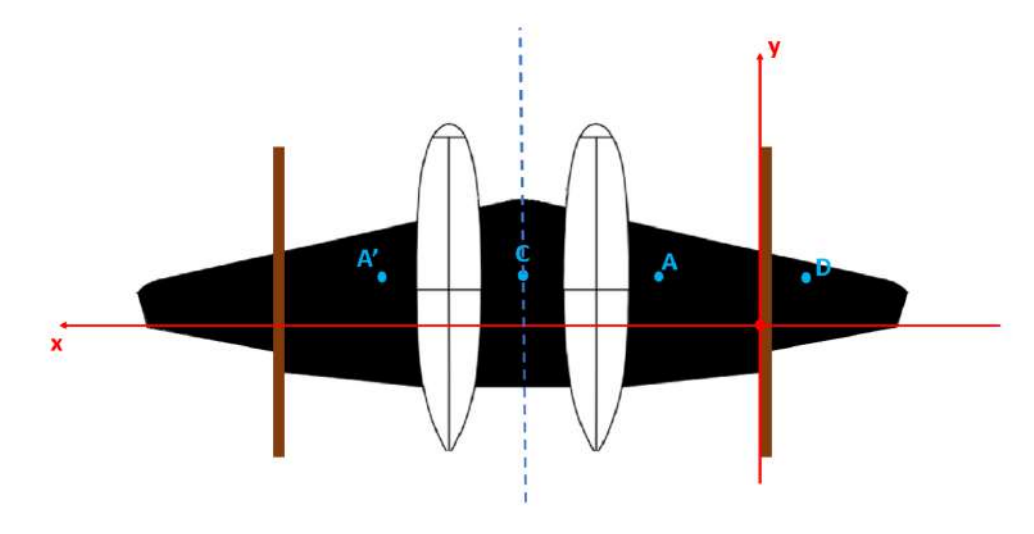


Figure 6 – LVDT Positions During Static Validation Test

Displacements in vertical directions were measured throughout the experiment using LVDT transducers in the positions, shown in Figure 6. The results obtained from both the Nastran's SOL101 analysis and the experimental test can be visualized in the graphics, shown in Figure 7.

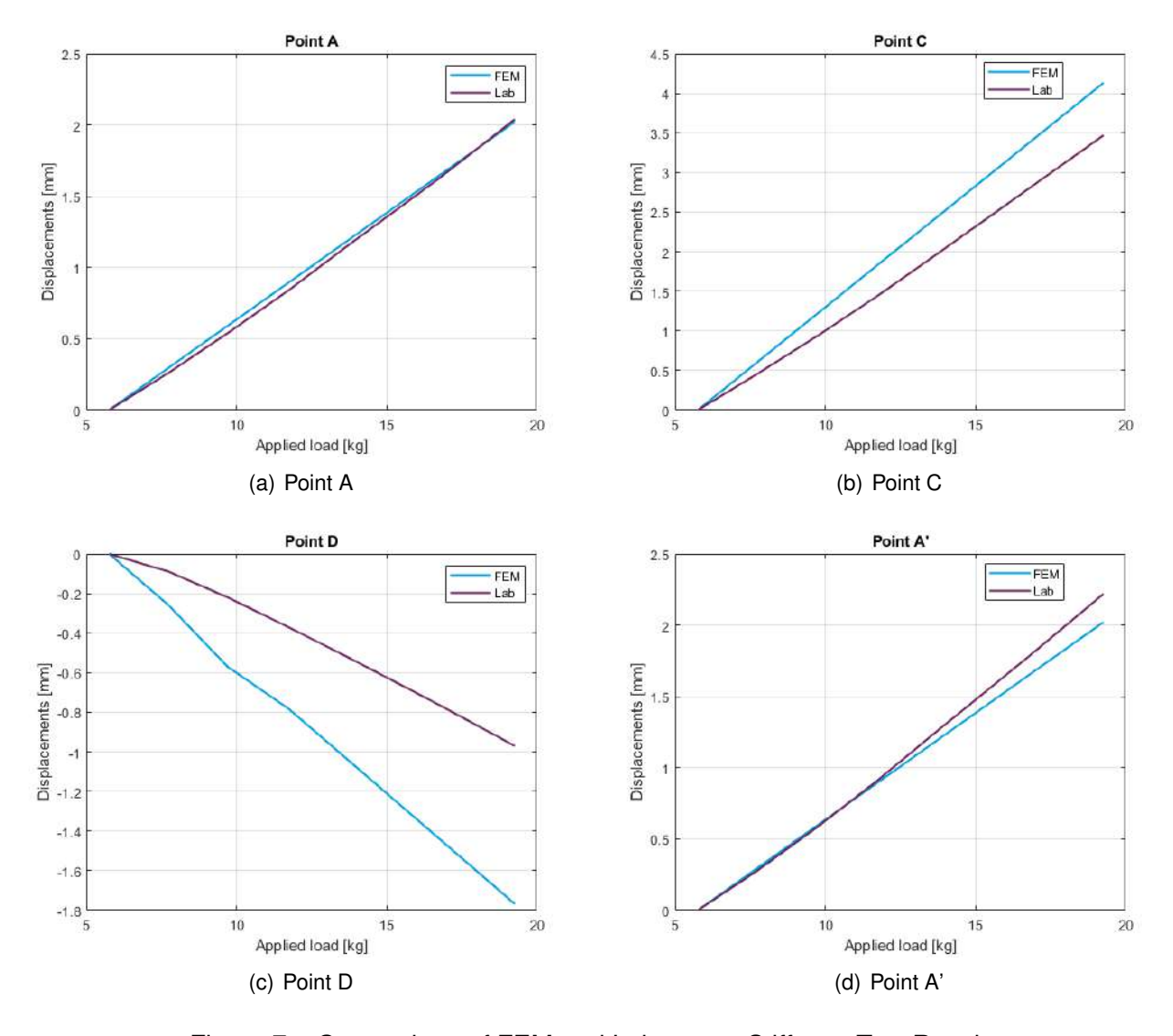


Figure 7 – Comparison of FEM and Laboratory Stiffness Test Results

The comparison between the results confirmed the match between the model and the real seaplane on a static level, except for Point D performances. The differences regarding this measure can be explained with an improper placement of the LVDT sensor that measures displacements. The sensor is probably not perfectly perpendicular to the surface in that point so it measures a lower displacement.

Static behaviour confirmed, other kinds of tests can now be executed in order to obtain a more enhanced understanding of the seaplane, under different conditions.

2.2 Non-Structural Masses Modelization

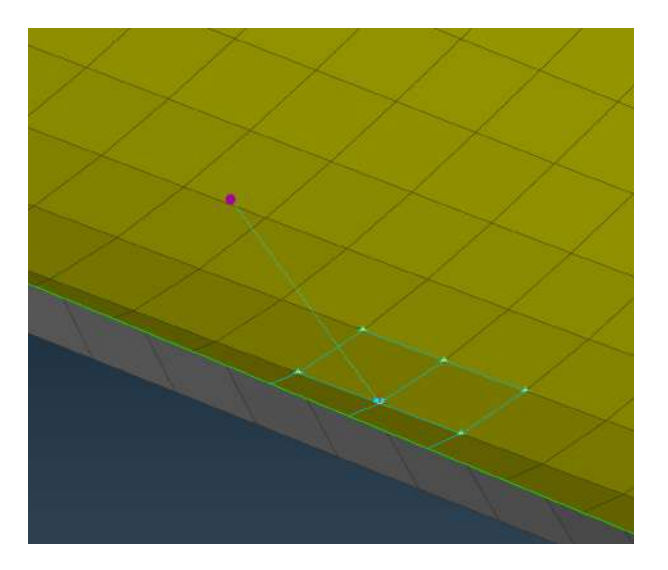


Figure 8 – Concentrated Mass Simulating the Left Wing Receiver

To determine the modal shapes of the seaplane, it is necessary to incorporate non-structural masses into the finite element (FE) model. Due to the small size of these masses, they can be accurately represented as concentrated masses. In order to achieve this, all the system masses are mapped, and the coordinates of their centers of gravity are identified. A node is then created at each center of gravity and a CONM2 element is assigned to it. The CONM2 element simulates a concentrated mass, with each CONM2 element representing the mass of the corresponding system component. Finally, the created node is connected to the appropriate nodes of the seaplane's structural components using an RBE2 rigid connection (Figure 8).

2.3 Analysis Parameters Settings

Modal shapes and vibration frequencies are calculated using Nastran's SOL103. Since the goal is to reproduce experimental free-free test, no constraints and no forces are applied to the seaplane. Since the model has numerous elements (362921 shell elements) a lumped mass matrix is used to reduce computational cost.

For the eigenvalue extraction Lanczos method is selected.

3. FEM results

The numerical analysis executed using the FEM model allowed us to calculate modal shapes and identify those at which significant structural responses are manifested. The first two global shapes are chosen to be verified by the experimental tests. In Table 2, frequencies regarding first and second bending behaviors are shown.

Modes	Vibrational Frequencies [Hz]
I Bending	20.7
II Bending	43.1

Table 2 – Vibrational Frequencies Referred To The Numerical Analysis

The Figures 9 and 10 represent the modal shapes obtained through the FEM Analysis.



Figure 9 - Frequency: 20.7 Hz - I Bending



Figure 10 - Frequency: 43.1 Hz - II Bending

4. Ground Vibration Test

To validate the data obtained theoretically through the finite element model, an experimental test is conducted to verify the operational deformations of the aircraft [9] [10].

4.1 Setup

For the execution of the test, the following materials are required:

- · Six elastic ropes;
- · Eight hooks;
- · Polytec PSV-500 laser vibrometer;
- TMS K2007E01 shaker;
- · An alluminium support structure;
- Sheet of reflective tape.

It is planned to suspend the aircraft to simulate free-free constraints using elastic ropes. These ropes are composed of the components shown in the Table 3.

Name	Quantity	Length [m]	Diameter [mm]	Strength [N]
Elastic rope	6	8.5	8	950
Hook	8	0.073	4	-

Table 3 – Ropes

The ropes are then secured to a grid located 4 meters above the ground using the previously described hooks.

The aircraft is kept in a vertical position (Figure 11), with the leading edge of the wing maintained at approximately one meter above the floor.



Figure 11 - Elastic Ropes Setup

To maintain this position, four ropes are placed around the leading edge of the wing, specifically two internally and two externally the hulls. The remaining two ropes are inserted between the engine frame beams and kept taut towards the floor; these serve to minimize the oscillations of the aircraft. To avoid damaging the leading edge, it was decided to insert a sheet of breather material between the ropes and the trailing edge.

4.2 Instrumentation

Due to the execution of the test, two instruments were indispensable: the shaker and the Laser Doppler Vibrometer. The first instrument allowed us to create the correct environment to execute the test, and the second one simultaneously provided us with the opportunity to capture the results and, afterwards, analyze them.

4.2.1 Shaker

To apply vibration to the object under analysis, a decision is made to utilize a shaker, specifically a permanent magnet shaker, capable of delivering impulses with frequencies up to 9 kHz [8]. This decision is made to conduct the test while maintaining control over the excitation signal. The intended frequency range for the test is 0-125 Hz.

In Figure 12, an image of the shaker and its setup during tests is shown. By varying the intensity of the current flowing through the shaker coils, it is possible to provide a precise type of excitation:

- · Sinusoidal;
- · Random;
- · Periodic;
- · Transient.

During the test in question, a periodic excitation was used.

The excitation is transferred from the shaker along its axis to the aircraft using a rod called a "stinger", a nylon rod that is not very rigid in the transverse direction to avoid unwanted stiffness, as it can be assimilated to a constraint.

At the end of the stinger, there is a load cell, which is necessary for monitoring the force of the impulse transmitted by the shaker. At the free end of the load cell, a striker is mounted, which was placed in contact with the wing section.



Figure 12 – Shaker Setup

4.2.2 Laser Vibrometer

In a laser vibrometer, the system operates by alternating roles between the receiver and the source, creating a complex interaction. Initially, the moving object acts as the receiver of the laser beam emitted by a fixed source. When the laser beam is reflected back, the roles reverse: the vibrating object becomes the source of the laser beam, which is then received by the fixed sensor (Figure 13).

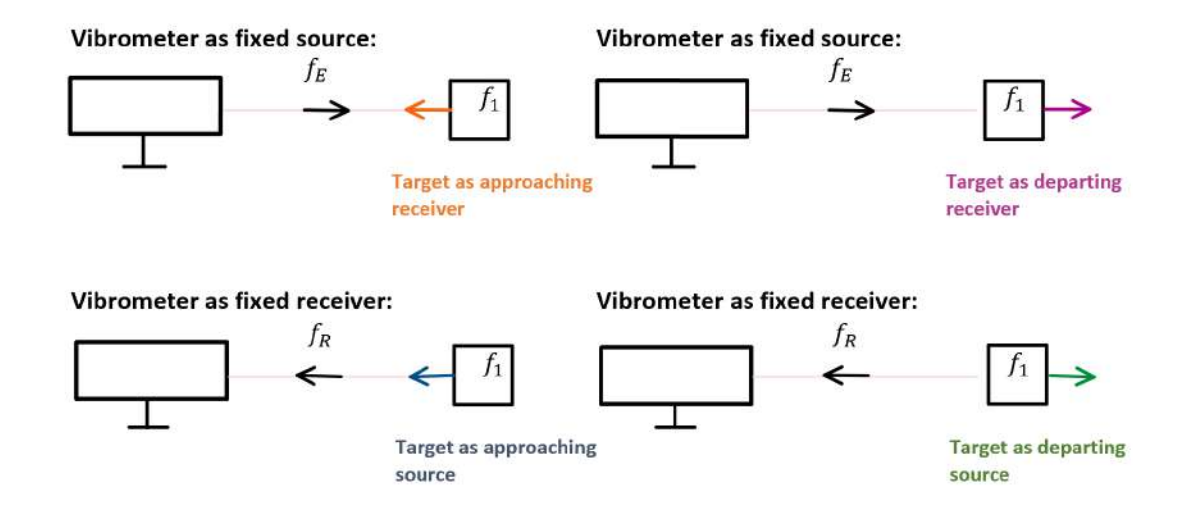


Figure 13 – LDV Operating Principle

When the object moves towards the laser, the laser emits light at a frequency f_e . The object, acting as a receiver, perceives this light at an apparent frequency f_1 , which is adjusted according to the Doppler effect formula for a stationary source and a moving receiver. Upon reflecting the light, the object now acts as a moving source with frequency f_1 , and the fixed receiver perceives the light at a modified frequency. Ultimately, the difference between the received and emitted frequencies equals twice the vibration velocity (v) divided by the laser beam's wavelength (λ) :

$$f_R - f_E = \frac{2\nu}{\lambda} \tag{1}$$

with

$$f_R = \frac{c}{c - v} \times f_1 \tag{2}$$

the frequency detected by the vibrometer. Conversely, if the object moves away, the final formula is reversed.

This theoretical framework underpins the operation of laser vibrometers. However, these formulas hold true only when the laser beam is parallel to the direction of motion, which is often not the case in practical applications. As a result, a directional vector is introduced into the formula, causing a cosine error. In the case of a small vibrometer, a test setup can be constructed to minimize this error by aligning everything perpendicularly. For more complex setups, this alignment is achieved only at a single point, as the laser beam is sequentially redirected by scanning mirrors to various measurement points, making the initial condition valid only at the starting point. Nevertheless, the software compensates for these cosine errors.

The laser vibrometer considered for the measurements is the PSV-500-B model (Figure 14), and it consists of the following elements [5] [6]:

- · Scanning head;
- · Front end;
- · Industrial PC.

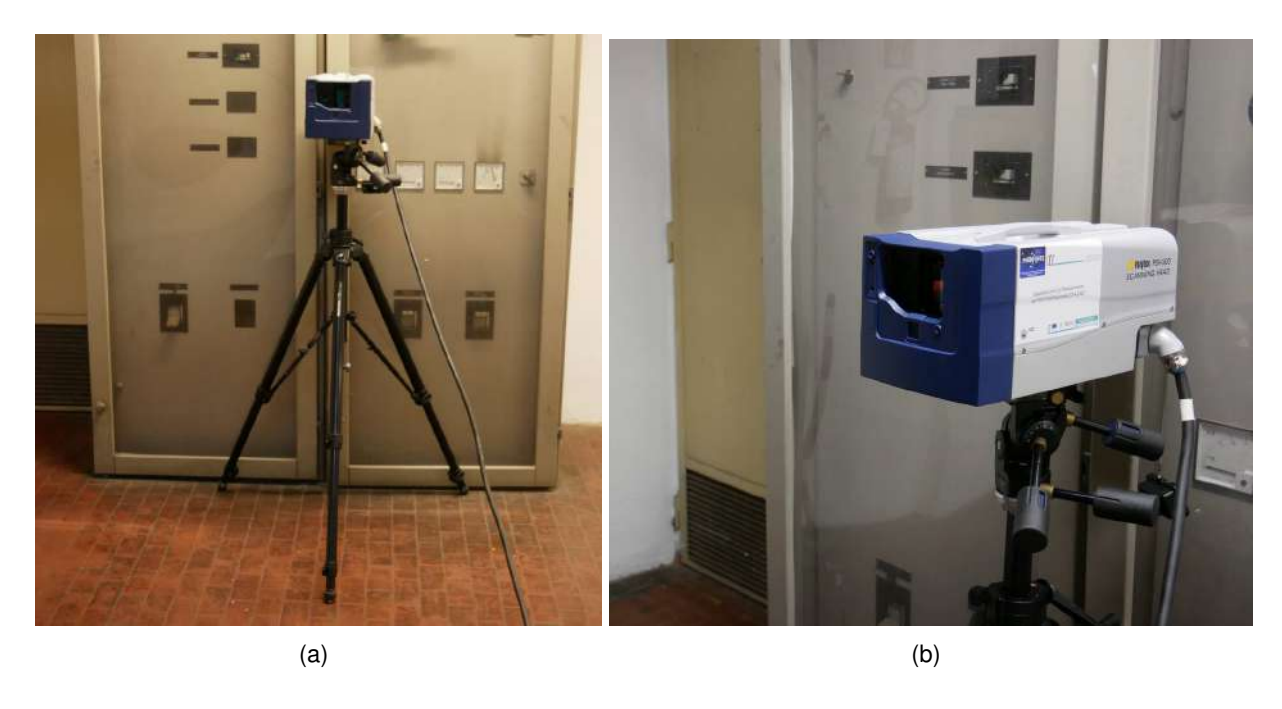


Figure 14 – Laser Vibrometer

After positioning the instrument and turning on the computer, the measurement preparation phase is initiated, enabling the use of the software through the following steps [7]:

- 2D Alignment: the system aligns the camera with the laser position;
- Scanning Grid Definition: a grid of virtual points of the object under analysis is created;
- Autofocus: enhancing reflectivity by optimizing individual focus values. The optimal focus is calculated only for certain points, with the focus value of others being interpolated;
- · Acquisition Settings Configuration;
- Measurement: the system sends the signal to the shaker and automatically scans the grid;
- Results Analysis: visualization of operational deflections.

This instrument is placed at a distance of 4.62 meters from the model. This distance allows the laser to cover an area corresponding to the entire wing surface, given the scanning angle of 40°. The Laser Vibrometer should be positioned along the symmetry axis of the aircraft, so that it is centered respect to the area being examined.

It is crucial that the distance at which the laser is positioned adheres to a specific law, which highlights that within certain distance ranges, the signal is more favorable compared to others. This can be visualized in Figure 15, as with the following formula [6]:

$$Optimal\ stand - off\ distance = 141mm + (n \cdot l)$$
(3)

with

$$n = 0, 1, 2, \dots$$
 (4)

$$l = 204mm \pm 1mm \tag{5}$$

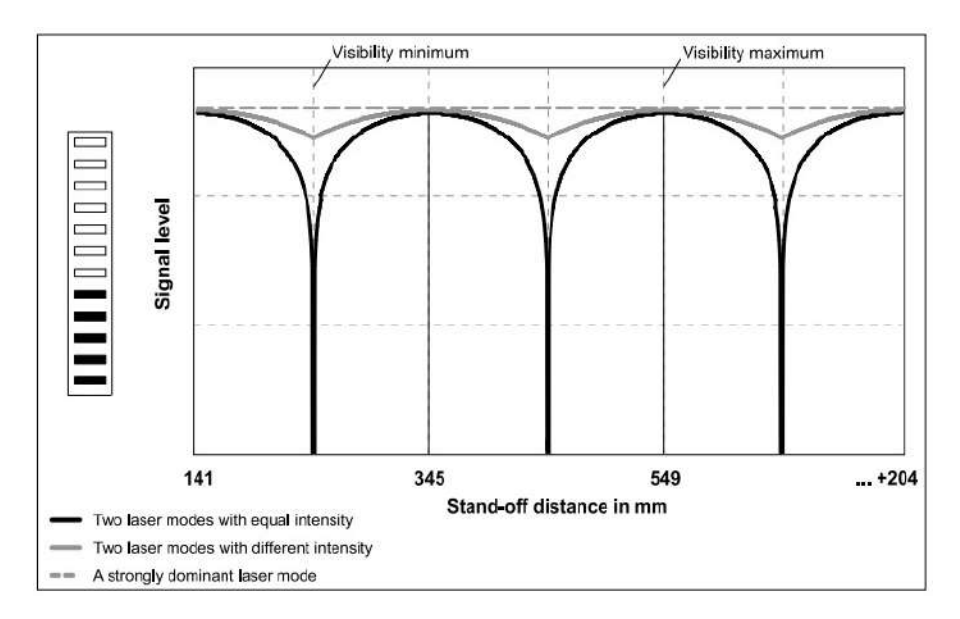


Figure 15 – Relation Between Stand-Off Distance and Signal Level [6]

The chosen distance falls within the prescribed range to ensure accurate measurement.

4.3 Procedure

The test was conducted by analyzing only the dorsal surface of the aircraft. Before conducting the test, it is important to pay attention to the following recommendations:

- The area should have controlled lighting, meaning it should not be too bright or too dim;
- During the test, do not stand close to the laser vibrometer, as this will alter the measurements;
- The ropes should not be taut, as this would allow vibrations to pass through them to the grid and reflect back, affecting the shaker's impulse. Therefore, it is essential that the ropes are as relaxed as possible.

The Chain of Measurement [11] is illustrated in the Figure 16.

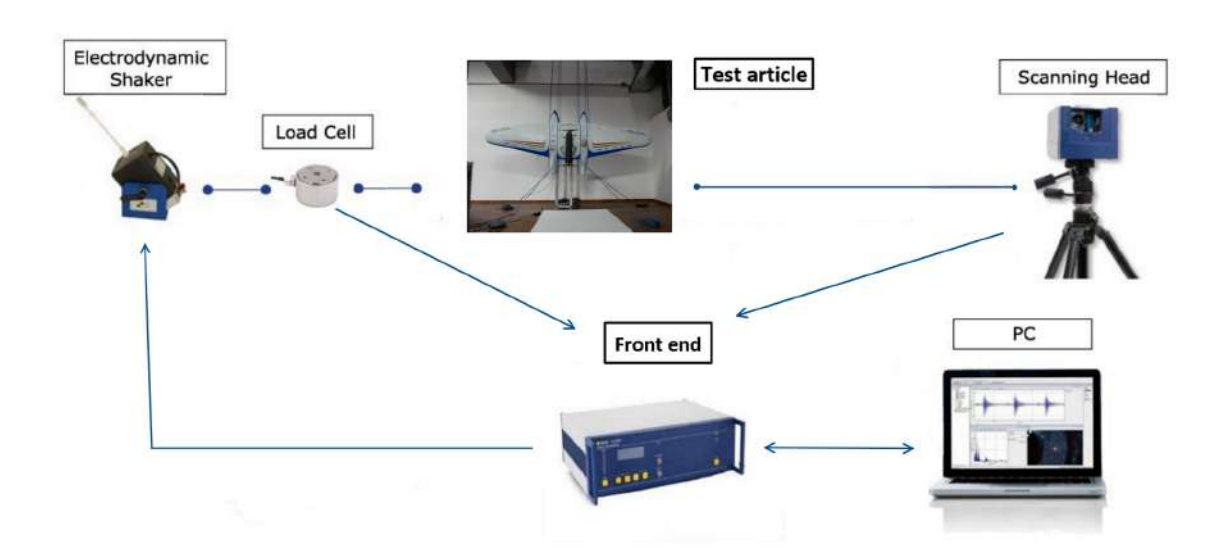


Figure 16 - Chain of Measurement

The test execution procedure is summarized in the following steps:

1. Suspending the Test Article:

- Place four elastic ropes to suspend the Test Article in mid-air and the remaining two ropes to prevent the oscillations of the aircraft, as shown in section 4.1;
- Ensure the leading edge of the aircraft is about one meter above the ground.

2. Choosing measurement points:

• Choose measurement points on the aircraft dorsal surface and apply a piece of reflective tape to improve reading of the surface.

3. Positioning the Shaker:

- Place the shaker on the aluminum support structure to achieve the correct height;
- Place the shaker in contact with the underside of the aircraft, ensuring that the stinger is perpendicular and at the center of the central wing box.

4. Setting Up the Laser Vibrometer:

• Set up the laser vibrometer as described in section 4.2.2 .

5. Setting up the software:

- Start the data acquisition software;
- Perform 2D alignment within the software to align the image seen by the laser vibrometer with that of the software;
- Set the measurement points corresponding to where the reflective tape was applied, monitoring the signal strength for each point, and create a grid of triangular areas to simulate the surface.

6. Acquisition settings:

- Choose the Periodic Chimp as pulse type to analyze all frequencies in the range of 0-125 Hz;
- Set a pre-trigger to avoid starting the measurement of a specific point below a minimum value, to avoid having false measurements, thereby achieving better results;
- Set the shaking speed of the shaker.

7. Starting the analysis.

8. Displaying results through graphs and animations.

5. Experimental Results

Following the execution of the procedure and the measurements, the results are analyzed.

The operational deflections derived from the results are illustrated in Figures 17 and 18. These correspond to the following frequencies measured by the instrument:

- 19.5 Hz, which corresponds to the first bending mode.
- 42.5 Hz, which corresponds to the second bending mode.

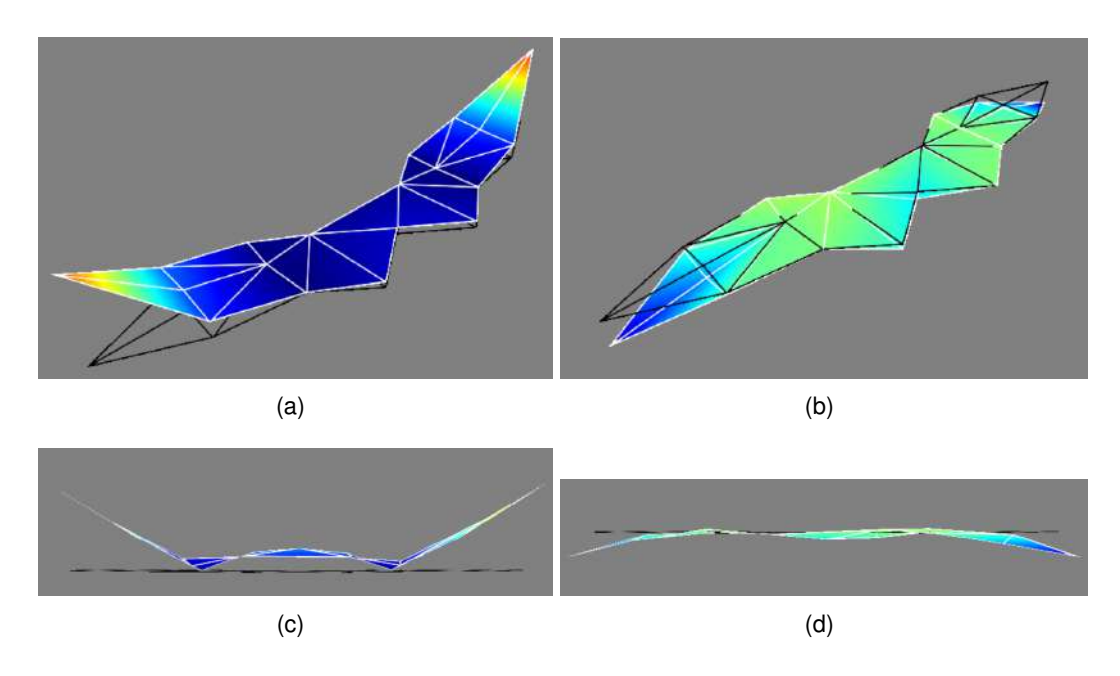


Figure 17 – Frequency: 19.5 Hz

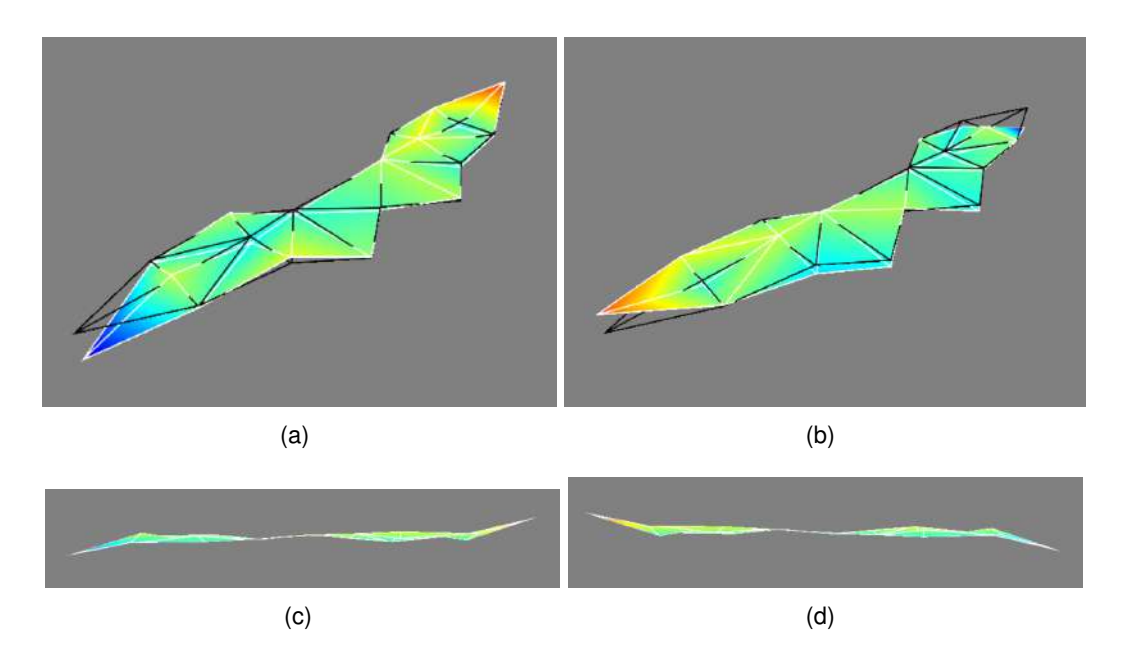


Figure 18 – Frequency: 42.5 Hz

These frequencies were extracted from the frequency response spectrum shown in Figure 19.

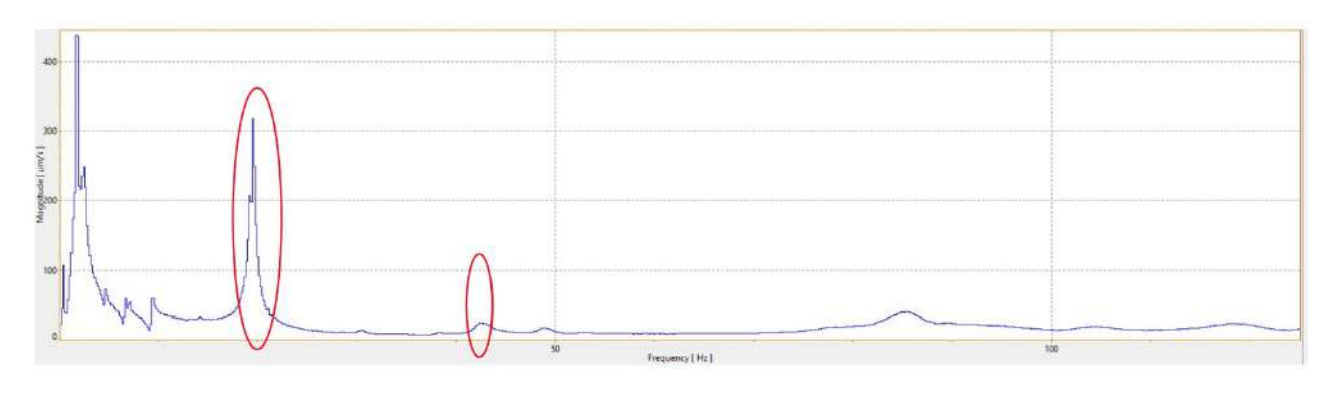


Figure 19 – Frequency Response

The first peak observed in the graph corresponds to the rigid modes, as indicated by its very low frequency. Therefore, this peak was disregarded in the results.

6. Numerical and Experimental Comparison

Primarily, it is essential to verify that the masses simulated in the FE model represent correctly the test article mass. The masses of the individual parts are given in the Table 4.

Component	Quantity	Mass [kg]
Wing ribs	12	0.266
Wing spars	4	0.393
Skin wing	1	3.017
Frames	6	0.251
Fuselage spars	2	0.131
Skin fuselage	1	3.824
Battery compartment	2	0.168
Wingbox ribs	6	0.543
Wingbox spars	4	0.289
Wingbox skin	1	1.259
Paint	1	0.240
Engine mount	1	2.481
Engine mount supports	6	0.325
Batteries	8	7.002
Other non-structural masses	62	2.247

Table 4 - Masses of individual components

In Table 5 a comparison between the test article's mass and the calculated FE model one is shown.

	FE Model	Test article	Relative error
Mass [Kg]	22.44	23.08	2.8 %

Table 5 – Mass Comparison

Since the error between the masses is considered acceptable, it is possible to proceed with the comparison of the modal frequencies and shapes:

	FE Model Frequencies [Hz]	Test Frequencies [Hz]	Relative Error
Mode 1	20.7	19.5	6.2 %
Mode 2	43.1	42.5	1.4 %

Table 6 - Frequencies Comparison

In Table 6 frequencies of the first three global modes of the seaplanes are shown. The error proves di FE model correct as it is furthermore demonstrated by the modal shapes results shown in sections 5 and 3.

The errors can be explained as follows:

- It is impossible to replicate a free free condition. The rubber bands have eigenfrequencies that
 are way lower than the seaplane ones so they do not interfere with their calculation but they
 might have a slight impact on the modal shapes;
- It is really difficult to constrain roll rotations of the seaplane so it is possible that a rigid body movement in this directions happens damaging a little final results;
- The seaplane is manufactured using composite materials with hand lay-up technique so it is really difficult to numerically characterize its mechanical and inertial properties with very high accuracy;
- Non structural mass simulation using 0D elements surely introduces errors.

Despite the acceptable errors the results show great compatibility between the FE model and the test results so now the model can be considered validated on a static and dynamic level.

7. Conclusions

In conclusion, it is important to summarize the main advantages and disadvantages of using a laser vibrometer to test a structure.

The most noticeable advantages are:

- It is possible to track a very high number of structure points with a simple experimental set-up. In a classic set-up in which the measurements are taken by accelerometers, it is necessary to apply one detector and everything connected with it at each point. In this experiment 19 points are tracked which means that in a more classic set-up 19 accelerometers and 19 cables must be applied and managed. It is therefore possible to perform tests in significantly less time;
- With the right setup configuration and a proper illumination, the laser enables high-precision
 measurements in a relatively shorter time compared to other methods for performing the same
 test. The ability to quickly and accurately capture vibration data not only enhances productivity
 but also ensures the reliability and consistency of the results;
- The laser has no mass so it does not interfere in any way in the modal response of the structure.
 This advantage may appear not important with structures with high mass like the seaplane here analysed, but it becomes relevant with extremely lightweight structures. In this last case the application of accelerometers can completely distort the results.

The main disadvantage, except for the economic implications of this kind of instrument, is that it is necessary to replicate the test multiple times to set up correctly all the parameters in order to obtain clean results. Even so the overall time needed to set-up and conduct the tests is still lower than the one used with more traditional sensors and the obtained results are more accurate and complete. Another disadvantage is that the setup needs to be changed to catch other vibrational modes, such as in-plane, torsional and axial.

8. Aknowledgments

The authors would like to thank the companies and people who contributed to this paper and to the 1:8 scale replica of the S55X. First of all, the entire Team S55, made up of young students full of enthusiasm, then Professor Enrico Cestino and Engineer Vito Sapienza, who constantly support the project by making their experience and time available to the team. We would also like to thank the Politecnico di Torino which has been supporting the team financially since 2017 investing in our projects. Moreover, thanks to all the companies and organisations that collaborate with the Team S55: Replica 55, Ellena-SPEM, BETA CAE Systems, Altair Engineering, HPC Polito, Siemens, Mike Compositi, Erreti Compositi, Enginsoft S.p.A and Ansys Inc. Last but not least, the authors express their gratitude to Dr. Matteo Sorrenti for assisting with the experimental setup.

9. Contact Author Email Address

Mail to:

Team S55: teams55.polito@gmail.com **Lovero F.:** s310100@studenti.polito.it

10. Copyright Statement

The authors confirm that they, and/or their company or organization, hold copyright on all of the original material included in this paper. The authors also confirm that they have obtained permission, from the copyright holder of any third party material included in this paper, to publish it as part of their paper. The authors confirm that they give permission, or have obtained permission from the copyright holder of this paper, for the publication and distribution of this paper as part of the ICAS proceedings or as individual off-prints from the proceedings.

References

- [1] Di Ianni L¹, Loiodice L¹, Celestini D¹, Tiberti D¹, Baldon C¹, Iavecchia P¹, Saponaro Piacente A¹, Prodan M¹, Grendene S¹, Barberis B¹. and Santoro L¹, ¹Politecnico di Torino, Italy, Team S55: 1:8 scale "replica" of the SIAI-MARCHETTI S55-X, 32nd ICAS 2018 Congress, 6-10 September 2021, Shanghai (China)
- [2] Cestino E¹, Frulla G¹, Sapienza V¹, Pinto P¹, Rizzi F¹, Zaramella F.¹ and Banfi D. ¹ "REPLICA 55 PROJECT: a wood seaplane in the era of composite materials", *31st ICAS 2021 Congress*, 9-14 September 2018, Belo Horizonte (Brasil)
- [3] G. Nicolosi¹, A. Lunghitano¹, S. Lombardi¹, T. Talamucci¹, A. Caivano¹, N. Simone¹, E. Cestino¹, V. Sapienza, Aeronautical Engineering Consultant, Italy; ¹Politecnico di Torino, Italy. "WING STATIC STRUCTURAL ANALYSIS AND EXPERIMENTAL TESTING OF A COMPOSITE 1:8 S55-X REPLICA". 33nd ICAS 2022 Congress, 4-9 September 2022, Stockholm (Sweden)
- [4] Cusano A., Capoluongo P., Campopiano S., Cutolo A., Giordano M., Felli F., Paolozzi A., Caponero M. "Experimental Modal Analysis of an Aircraft Model Wing by Embedded Fiber Bragg Grating Sensors". *IEEE Sensors Journal, Volume 6, Issue 1, February 2006*
- [5] Polytec Datasheet PSV-500 https://www.acoutronic.eu/pdf/vibration/Polytec Datasheet PSV-500.pdf
- [6] Polytec Operating Instructions PSV-500 https://www.polytec-cn.com/uploads/ueditor/20190719.pdf
- [7] Polytec_Software_Manual_Polytec_Update_1.1 https://www.polytec.com/int/vibrometry/products/software
- [8] Mini Smart Shaker with Integrated power Amplifier https://www.atecorp.com/atecorp/media/pdfs/data-sheets/modal-shop-2007e_datasheet.pdf
- [9] Dennis Göge, Marc Böswald, Ulrich Füllekrug, Pascal Lubrina. "Ground Vibration Testing of Large Aircraft-State-of-the-Art and Future Perspectives". https://www.researchgate.net/publication/338690769_Ground Vibration Testing of Large Aircraft State of the Art and Future Perspectives
- [10] What is Ground Vibration Testing? https://boomsupersonic.com/flyby/what-is-ground-vibration-testing
- [11] Cesare Patuelli, Alessandro Polla, Enrico Cestino, Giacomo Frulla. "Experimental and Numerical Dynamic Behavior of Bending-Torsion Coupled Box-Beam" https://link.springer.com/article/10.1007/s42417-022-00759-7